Title

Intracranial electrical stimulation of corticolimbic sites modulates arousal in humans.

Authors

Fan, Joline

Lee, A

Sellers, Kristin

et al.

Intracranial electrical stimulation of corticolimbic sites modulates arousal in humans

Joline M. Fan[a,b,*], **A. Moses Lee**[b,c], **Kristin K. Sellers**[b,d], **Kai Woodworth**[b,c], **Ghassan S. Makhoul**[b,c], **Tony X. Liu**[b,c], **Catherine Henderson**[b,c], **Daniela A. Astudillo Maya**[b,c], **Rebecca Martinez**[b,c], **Hashem Zamanian**[b,c], **Benjamin A. Speidel**[a,b], **Ankit N. Khambhati**[b,d], **Vikram R. Rao**[a,b], **Leo P. Sugrue**[b,c,e], **Katherine W. Scangos**[b,c], **Edward F. Chang**[b,d], **Andrew D. Krystal**[b,c]

[a]Department of Neurology, University of California, San Francisco, CA, USA

[b]Weill Institute for Neurosciences, University of California, San Francisco, CA, USA

[c]Department of Psychiatry and Behavioral Sciences, University of California, San Francisco, CA, USA

[d]Department of Neurosurgery, University of California, San Francisco, CA, USA

[e]Department of Radiology, University of California, San Francisco, CA, USA

Abstract

Background: Humans routinely shift their sleepiness and wakefulness levels in response to emotional factors. The diversity of emotional factors that modulates sleep-wake levels suggests that the ascending arousal network may be intimately linked with networks that mediate mood. Indeed, while animal studies have identified select limbic structures that play a role in sleep-wake regulation, the breadth of corticolimbic structures that directly modulates arousal in humans remains unknown.

Objective: We investigated whether select regional activation of the corticolimbic network through direct electrical stimulation can modulate sleep-wake levels in humans, as measured by subjective experience and behavior.

*Corresponding author. University of California, San Francisco, Department of Neurology and Weill Institute for Neurosciences, 505 Parnassus Ave, Box 0114, San Francisco, CA, 94158, USA. Joline.Fan@ucsf.edu (J.M. Fan).

Methods: We performed intensive inpatient stimulation mapping in two human participants with treatment resistant depression, who underwent intracranial implantation with multi-site, bilateral depth electrodes. Stimulation responses of sleep-wake levels were measured by subjective surveys (i.e. Stanford Sleepiness Scale and visual-analog scale of energy) and a behavioral arousal score. Biomarker analyses of sleep-wake levels were performed by assessing spectral power features of resting-state electrophysiology.

Results: Our findings demonstrated three regions whereby direct stimulation modulated arousal, including the orbitofrontal cortex (OFC), subgenual cingulate (SGC), and, most robustly, ventral capsule (VC). Modulation of sleep-wake levels was frequency-specific: 100Hz OFC, SGC, and VC stimulation promoted wakefulness, whereas 1Hz OFC stimulation increased sleepiness. Sleep-wake levels were correlated with gamma activity across broad brain regions.

Conclusions: Our findings provide evidence for the overlapping circuitry between arousal and mood regulation in humans. Furthermore, our findings open the door to new treatment targets and the consideration of therapeutic neurostimulation for sleep-wake disorders.

1. Introduction

Humans routinely shift their arousal levels in response to mood, stress, and reward [1-3], complementing internal homeostatic and circadian drives. For example, stressful stimuli that give rise to aversive or rewarding outcomes may promote increased vigilance and wakefulness, whereas less motivating stimuli, such as a monotonous lecture, can lead to decreased vigilance and increased sleepiness. Furthermore, in many disorders of mood, e.g. depression, anxiety, and mania, maladaptive responses to emotional factors can lead to disruptions in the control of sleep and wakefulness [4-7]. Nearly 90% of patients with depression are reported to have sleep-wake disturbances, including insomnia and hypersomnia. The diversity of emotional factors that modulates arousal in both adaptive and maladaptive ways suggests that the arousal circuitry may be more distributed than previously appreciated and integrated into the networks that mediate mood. In this study, we tested the hypothesis that regional activation of corticolimbic network sites differentially modulates sleep-wake level by measuring behavioral stimulation-responses in human participants. If sleep-wake levels can be differentially modulated through stimulation of corticolimbic circuitry, this may support a circuit mechanism for the adaptive fluctuations of arousal that occur in healthy individuals to emotional stimuli or the sleep-wake dysfunction that occur in individuals with mood disorders [6,7]. Furthermore, it may support specific corticolimbic regions as treatment targets for the consideration of neurostimulation therapies for intractable sleep-wake disorders.

Indeed, the current conception of arousal networks has extended beyond classical structures (e.g. brainstem, hypothalamus, and basal forebrain) to include distributed pathways of the ascending arousal system, including within limbic structures [8-12]. Dating back to the 1950s, regional limbic activation, such as with the direct stimulation of the amygdala [13]

or mesial temporal lobe seizures [14], was identified to elicit a diffuse cortical arousal pattern of low-amplitude fast activity, reminiscent of the activation of the brainstem reticular system, albeit with complex clinical features. The amygdala was subsequently implicated in the cortical synchronization of low-gamma activity, enabled by its widespread reciprocal connections with the cortex [15]. More recently, electrical and optogenetic neuromodulation of subcortical regions that have traditionally been implicated in reward or stress response, including the ventral tegmental area (VTA) [16-19] or bed nucleus of stria terminalis (BNST) [20], have been shown to promote sleep-wake transitions. In addition to circuit level behavioral studies, decades of psychometric research have led to the dissection of emotion into two dimensions of valence and arousal [21-24], implicating the coregulation of mood and arousal networks. Yet, the extent to which subjective experience of arousal can be modulated at the level of mood circuits remains unclear.

Human studies may offer increased sensitivity for measuring fluctuations in arousal with direct neurostimulation through quantifying subtle changes in experience or function, rather than relying on isolated electrophysiologic changes and/or gross behavioral-state changes, e.g. the transition from sleep to wake. In fact, modulation of arousal in humans has been investigated using deep brain stimulation (DBS) techniques. However, these case-series were largely performed in cohorts with impaired consciousness, such as in patients with severe traumatic brain injury or stroke, and thus outcome measures were restricted to gross behavioral observations [25-27]. In addition, anatomical targets to-date have been limited to structures long identified as playing a role in sleep/wake regulation, including the pedunculopontine nucleus (PPN), medial thalamus, basal forebrain, and hypothalamus, with variable success. Other studies in patients with advanced Parkinson's disease (PD) and severe sleep-wake disturbances demonstrated that low frequency stimulation of the PPN decreases daytime sleepiness [28,29], suggesting that there is an opportunity for modulating arousal in patients with less severe neurologic disease. Stimulation of downstream targets in subjects who are cognitively intact and can report experiential changes may allow for a more sensitive identification of arousal responses elicited by direct brain stimulation.

In this study, we hypothesized that sleep-wake level can be modulated by regional activation of the corticolimbic network, providing supporting, mechanistic evidence that the corticolimbic network may provide a parallel pathway for augmenting arousal. We tested this hypothesis by leveraging an ongoing clinical trial [30,31] focused on assessing the antidepressant effects of intracranial stimulation. By assessing subjective experience and clinical behavior, we performed mapping of sleep-wake responses to acute corticolimbic stimulation. Our findings reveal a set of corticolimbic targets, whereby stimulation differentially modulates sleep-wake levels and electrophysiologic biomarkers in the gamma band correlate with changes in arousal. These results provide new mechanistic support for the distributed circuitry of the arousal network across corticolimbic sites. These findings further support novel targets and the consideration of therapeutic neuromodulation strategies for the treatment of refractory sleep-wake disorders.

2. Methods

2.1. Participant cohort

The study design leveraged an ongoing in-hospital clinical trial (NCT04004169) involving the implantation of intracranial electrodes in participants with treatment-resistant depression [30]. Participants included in the study were required to have treatment-resistant depression without suicidality and prior successful but transient response to electroconvulsive therapy (ECT). During the hospitalization, no sleep-wake medications, including stimulants or sedatives, were administered during or within 10 h prior to the testing period. Two patients (a 31 year-old Caucasian man and a 29-year old Caucasian woman) met inclusion criteria and were implanted with multi-site, intracranial depth electrodes and underwent a 10 d period of intensive stimulus response mapping in the UCSF Epilepsy Monitoring Unit [30]. Neither participant was previously formally diagnosed with a sleep-wake disorder; however, Patient 2 had required stimulants as needed for symptoms of daytime sleepiness and zolpidem as needed for insomnia. In addition, Patient 2 had been maintained on nightly trazodone for symptoms of both mood and insomnia.

2.2. Electrode placement, reconstruction, and tractography

Sixteen-contact depth electrodes (PMT® sEEG Depthalon electrodes, 3.5 mm pitch, center to center) were implanted in the two patients enrolled in the inpatient study. Electrodes were implanted using standard neurosurgical techniques with trajectories targeting the bilateral amygdala (Amy), hippocampus (Hipp), subgenual cingulate (SGC), orbital frontal cortex (OFC), and ventral capsule (VC) with the most distal contacts. Due to differences in electrode trajectories based on individual neuroanatomy, Patient 2 also had left nucleus accumbens (NAC) represented. All subjects underwent presurgical 3 T brain magnetic resonance imaging (MRI), including 1 mm isotropic T1-and T2-weighted imaging, and post-operative computed tomography (CT) scan for electrode localization. Electrode locations were determined by coregistering the presurgical T1-weighted MRI sequence with the post-operative CT. Anatomical locations of each electrode were determined by neuroradiologist review (L.P.S.).

Fiber tracts were identified using the Lead DBS toolbox [32] in MATLAB (Mathworks, Inc., Natick, MA). Pre-operative MRI and post-operative CT scans were co-registered and normalized to a standardized Montreal Neurological Institute template (MNI152, ICBM 2009b NLIN asymmetric) [33]. Putative fiber tracts were derived from a normative group connectome based on 32 subjects from the Human Connectome Project (HCP) (as detailed in Horn et al., 2017 [34]) based on a simple spherical estimate of the volume of tissue activated by a 5 mA unipolar stimulation at the mean location between the individual electrode pair used for bipolar stimulation during the study (according to the stimulation model detailed by Dembek et al., 2017 [35]). For each participant and region, the electrode pair modeled represents the pair that was tested most frequently for that region.

2.3. Behavioral measures and responses

Three behavioral ratings were used to capture the degree of arousal of the patient. First, a visual-analog scale (VAS) was completed by the patient to rate the level of energy. The VAS

was presented to the patient as a digital slider scale with the level of energy anchored by 0 (i.e. "not at all energetic") and 100 (i.e. "very energetic"). Second, the Stanford Sleepiness Scale (SSS) [36], a validated, 7-point self-rated scale of sleepiness, was completed by the patient to determine the degree of sleepiness. Scores of SSS ranged from 1 ("Feeling active, vital, alert or wide awake") to 7 ("No longer fighting sleep, sleep onset soon, having dream-like thoughts"). Third, arousal metrics were scored by a bedside observer using a 5-point Likert scale ranging from −2 (i.e. episodes of eye closure, decreased responsiveness to the environment, slowed speech rate) to 2 (i.e. high level of engagement with the environment, completion of tasks, relatively rapid speech rate). Both participants were blinded to all simulation parameters for all survey assessments. In addition, arousal measures were obtained in a double-blinded fashion. Specifically, the bedside observer sat out of view from the streaming EEG.

At any time, patients were allowed to spontaneously report any experiences or symptoms. Verbal responses were not cued.

2.4. Stimulation paradigm and survey assessments during simulation

We note that the stimulation protocol employed in this study were originally designed for the treatment of depression; however, through these methods, it was possible to extract additional behavioral scores to evaluate sleep-wake responses to stimulation. As such, the regions that were repeatedly assessed and included in this study for each subject were found to have some degree of anti-depressant effects, and the frequency of stimulation at each region was a function of assessing antidepressant treatment potential for therapy. While this context led to a variation in the amount of data available for each stimulation site, this study offered the unique opportunity to elucidate subjective experience of sleep-wake effects in humans (without epilepsy and without the confounds of anti-seizure medication side effects), which is extremely rare.

Bipolar stimulation of adjacent or nearby electrodes and monitoring of real-time electrophysiologic data were performed using the Nihon Kohden System (Tokyo, Japan). Stimulation was performed on post-operative days 2 through 10 of the inpatient hospitalization for the two patients involved in the inpatient study. Bipolar stimulation was delivered with charge-balanced, biphasic, constant-current trains at a specified frequency, pulse width, and current. Bipolar contacts tested for each region and patient are listed in the Supplementary Materials (Table 1s). Intracranial EEG recordings were collected at 2–10 kHz sampling rates using the Nihon Kohden System and a secondary data stream.

Prior to experimental stimulation, a safety survey was first performed using short duration 1–3 s bursts of stimulation at all anatomically verified electrodes within candidate brain regions to assess for epileptiform discharges. Safety surveys were performed at 1 and 100 Hz, 100 μs pulse width, and increasing currents (1–6 mA). For each patient, brain regions and stimulation parameters that elicited epileptiform discharges were avoided in all subsequent experimental stimulation paradigms with longer-duration stimulation [37] (see Supplementary Methods).

During stimulation mapping sessions, participants were informed that stimulation would be performed at different brain regions but blinded to the location and parameters of the stimulation and the time when stimulation started and ended. Stimulation parameters varied by region and current (1–6 mA). All regions were tested at 100 Hz frequency; an additional frequency of 1 Hz was tested for the OFC contact, given a prior anti-depressant effect at low frequencies [30]. Sham (0 mA) stimulations were randomly included in a subset of the stimulation blocks to serve as an internal control. Baseline periods (i.e. no stimulation) were also interspersed throughout the stimulation testing period, as both a control condition and a source of resting-state data for the biomarker analysis (see below). Finally, washout periods of at least 2 min were included into the stimulation schedule to provide resting time for the participants to minimize carryover effects.

Participant surveys assessments were completed at the end of stimulation and baseline periods. To minimize survey fatigue, the frequency of survey assessments was reduced when consecutive stimulations were performed in the same brain region, for instance, with repeated intermittent stimulation paradigms and sequential escalations of stimulation current. To characterize responses of these stimulation paradigms, a single score was obtained, as detailed below. Bedside observer arousal scores were performed after each stimulation, including when participant survey responses were not administered.

2.5. Stimulation response analysis and statistics

Behavioral scores and survey responses were aggregated and visualized across regions of stimulation using MATLAB v2019a. As a subset of baseline recordings did not have bedside observer subscores, missing-data was predicted from a regression model using subjective energy and sleepiness measures as predictors for bedside arousal measures. Leave one-out-cross validation was performed to estimate the quality of the imputation (Supplementary Materials).

Stimulation responses were then collected across a range of stimulation paradigms during the 10d inpatient monitoring. Stimulation paradigms included single trial assessments (e.g. 90s continuous stimulation), sequential stimulation assessments (e.g. 90s continuous stimulation at 1 mA, 3 mA, then 6 mA), and intermittent stimulation assessments (e.g. 10s stimulation/60s off x 50 min).

For single trial assessments, stimulation responses were associated with the specifics of the stimulation, which varied by region and stimulation parameters, including current (0.5–6 mA), duration (30s-3min), and frequency (1Hz or 100Hz). During sequential stimulations, multiple current levels were tested sequentially while holding all other stimulation parameters constant, including electrode contacts, frequency, and duration of stimulation. To account for sequential stimulation results, the survey responses associated with the highest current level were included as a single point to summarize the series of tests. During intermittent stimulation paradigms, short duration stimulations followed by an off period were administered over a longer duration (e.g. 30–60 min). To account for intermittent stimulation results, the survey response with the highest deviation from baseline was included as a single point to summarize the overall response.

Principal component analysis (PCA) was performed across the behavioral outcome scores to provide a summary metric of arousal based on multiple subscores for each participant. To assess the significance of the behavioral responses, a two-sample Wilcoxon rank sum test was performed on the stimulation-response, summary arousal metrics against a null hypothesis of equivalence of baseline and sham testing. Statistical testing was thresholded for multiple comparison testing with false discovery rate (FDR) of 5%.

2.6. Biomarker preprocessing and statistical analysis

Resting-state electrophysiology and behavioral scores were collected throughout each testing day to capture baseline measures for biomarker analyses. Baseline measures were performed before stimulation testing or at least 10 min after the most recent stimulation to minimize the impact of stimulation on the biomarker recording of arousal. Survey assessments were obtained at the end of the baseline recording sessions. The intracranial electrophysiology data obtained over the 5 min prior to the initiation of the survey were used in biomarker development.

Offline analysis of electrophysiology data was performed in MATLAB v2019a and Python v3.10. Standard preprocessing of the data was performed, including common average referencing to the mean of all channels, down-sampling to 512Hz, and application of a notch filter to remove artifact from noise and harmonics (60Hz, 120Hz, 180Hz, and 240Hz). We employed a second-order IIR notch digital filter using the Scipy function scipy.signal.iirnotch and a frequency bandwidth of 2Hz above and below the filtered frequency (i.e. total of 4Hz band). Additionally, we performed visual identification and rejection of periods with artifact across all channels, rejection of channels with high degree of noise based on a kurtosis threshold, and band-pass filtering of 1–150 Hz.

Spectral power was obtained for individual channels using 25 scales with logarithmically increasing center frequencies between 1 and 150 Hz and by performing wavelet analysis with Morlet wavelets. Relative power was obtained by dividing the power associated with each scale by the total power (i.e. normalizing the power spectra for area under the curve to 1). The relative spectral power was then averaged across scales to arrive at average estimates within canonical frequency bands: delta (1–4Hz), theta (4–9Hz), alpha (9–13Hz), beta (13–31Hz), low gamma (31–81Hz), and high gamma (81–150Hz). Finally, the relative spectral power was averaged across the 5-min biomarker recording period and across channels within each anatomical region for statistical testing.

To assess the correlation between SSS and spectral biomarkers, Pearson's correlations were assessed across candidate regions and frequency bands. P-values were adjusted for multiple comparison testing with a FDR of 5% across all regions. SSS was selected as the behavioral outcome to enable a consistent metric for comparison across patients. Electrophysiologic biomarkers that were statistically significant in both patients were used as features of investigation in the Electrophysiology Response analysis described in the following paragraph. To further evaluate the biomarkers, the SSS ratings were divided into equal sized high and low sleepiness groups, i.e. a median split. Given that the patients substantially varied in their overall level of sleepiness, the threshold for high and low sleepiness group was patient-specific (Patient 1, high sleepiness state of   6 SSS; Patient 2,

high sleepiness state of 4 SSS). Logistic regression was performed to classify high and low sleepiness levels per patient based on six randomly selected features. Features with the highest predictive values were determined by mean F-values, following 1000 iterations of feature selection and logistic regression across different train-test splits. The top six features were recalculated in each iteration based on those with the highest F-score in a particular train set. Receiver operating characteristic (ROC) curves were constructed for the strongest logistic regression models to quantify the area under the ROC curve (AUC). Top F-score features were identified by calculating the percentage of the cross-validated models in which each feature was selected.

2.7. Electrophysiologic biomarker response to regional stimulation

To identify how local spectral power was affected by stimulation, spectrograms were constructed across candidate channels for each stimulation condition with 1) stimulation durations of 30s and 2) pre- and post-stimulation durations of 20s. Stimulation response was investigated on the narrow set of electrographic biomarkers that were identified to be significant across both patients in the Biomarker analysis. For processing stimulation response electrophysiology, spectral power was obtained by performing wavelet transform with the same center frequencies as above and averaged across electrodes representing individual regions. Averaged spectral power for pre-/post-stimulation were obtained using a buffer of 9s from stimulation, which was visually determined to avoid direct stimulation artifact. Specifically, to prevent the introduction of stimulation artifact to the analysis, the 9s periods acutely before and after stimulation were not included in the analysis; the buffer of 9s was conservatively determined by obtaining the maximum duration of stimulation artifact visualized within the channels and applying the rule symmetrically to both pre and post-stimulation analyses for all conditions (see Fig. 1s B,C,E,F tan blocks). Power was z-scored to the pre-stimulation period and subsequently smoothed using a 3s window size. Post-stimulation z-scored power was compared to pre-stimulation z-scored power, and the difference in pre- and post-stimulation spectral power were assessed by a two-sided, paired T-test, computed separately for each selected feature. Post-hoc multiple comparison thresholding with FDR of 5% was performed across the features investigated.

3. Results

3.1. Intracranial mapping to modulate arousal

Two patients underwent bilateral symmetric implantation of electrodes targeting candidate corticolimbic structures, followed by an intensive 10 d inpatient monitoring period, during which stimulation-response testing was performed (Fig. 1A). For each participant and region, the predicted volume of tissue activated by stimulation at the select electrode contact pair was used as a seed for fiber-tracking based on the normative connectome. We hypothesized that the resulting tracts reflect those most likely to be recruited by stimulation at the modeled electrode contact pairs. For the VC contacts, fibers belonging to the medial forebrain bundle (Patients 1,2; Fig. 1B, *top*), anterior thalamic radiations (Patients 1,2), and ansa peduncularis (Patients 1) were identified. For the SGC contacts, associated fiber tracts included the cingulum bundle (Patients 1,2; Fig. 1B, *middle*), forceps minor (Patient 2), and uncinate fasciculus (Patient 2). Finally, for the OFC contacts, associated fiber tracts included

the ventral component of the anterior thalamic radiations (Patient 1; Fig. 1B, *bottom*), uncinate fasciculus (Patient 2), and a branch of the frontal asalant tract (Patient 2).

Voluntary spontaneous remarks were made by Patient 1 during stimulation across the VC, amygdala, SGC, and OFC. While verbal responses were variable, notable example comments are presented in Fig. 2A. Patient 2 did not provide spontaneous remarks during stimulation, although they participated in frequent survey assessments. Quantitative outcome assessments (i.e. VAS energy, clinician-rated Likert arousal scale, and SSS) results from Patient 2 revealed increased energy (p = 0.002) and decreased sleepiness with right VC stimulation (p < 0.001), as well as decreased sleepiness with left OFC 100Hz stimulation (p < 0.001; Fig. 2A-C).

To best capture the regional stimulation response across all subscores, the quantitative behavioral assessments (i.e. arousal, SSS, and energy) were combined into a summary metric for each individual, corresponding to the first principal component (PC1) following dimensionality reduction with PCA. The contributions of each behavioral assessment to PC1 are provided in Table 2s. PC1 captured 83.0% and 79.7% of the variance in the data for Patient 1 and 2, respectively.

In both patients, right and/or left VC stimulation led to increased arousal/energy responses (Fig. 3; Patient 1, p < 0.001; Patient 2, left VC p = 0.019 and right VC, p < 0.001), as compared to the control. Statistically significant increases in arousal/energy were also observable in the right OFC 100 Hz (Patient 1, p = 0.001), left OFC 100 Hz (Patient 2, p = 0.008), and right SGC (Patient 1, p < 0.001). In addition, Patient 1 exhibited significant decreases in arousal with right OFC 1Hz stimulation (p = 0.011), an opposing effect as compared to 100 Hz stimulation within the OFC. Contralateral regions of stimulation, including left OFC 100 Hz and left OFC 1 Hz for Patient 1 and right OFC 100 Hz for Patient 2 were not statistically significant. Only regions that underwent three or more acute stimulation assessments were included in the stimulation analysis. There were no statistically significant differences in the time of day each stimulation was performed relative to the baseline condition (Fig. 2s A,B).

3.2. Biomarkers of sleepiness

To characterize electrophysiologic correlates of sleep-wake levels within the sampled regions, we then performed a biomarker analysis. Relative spectral power from resting-state recordings was correlated with patient-reported sleepiness levels (Fig. 4A; Patient 1, N = 59; Patient 2, N = 64). The top 20 regions and frequency bands whose spectral power levels are associated with high and low sleepiness for both patients are illustrated in Fig. 4B and C with the highest positive and negative correlations depicted in Fig. 4D and E. Across target regions, increased relative power in the low and high gamma frequency bands was associated with low sleepiness or high arousal/wakefulness (i.e. negative correlations with SSS), whereas increased relative power in the delta, theta, and alpha frequency bands was more commonly associated with increased sleepiness (i.e. positive correlations with SSS). The regions and features that are statistically significant across both patients are examined in the subsequent local electrophysiologic response analysis.

A logistic regression classifier was constructed to further characterize the ability of the spectral power features recorded from target regions to differentiate the dichotomous high or low sleepiness level for each patient. Utilizing the six top features most commonly selected across 1000 iterations of cross-validated feature selection, the AUC achieved was 0.75 for Patient 1 and 0.89 for Patient 2 (Fig. 4F and G). The top features determined for the logistic regression classifier for Patient 1 are the delta, alpha, and beta bands of the right hippocampus, the alpha and high gamma bands of the left VC, and the high gamma band of the right VC and bilateral OFC (Fig. 4G). The top features for Patient 2 are the high and low gamma bands of the bilateral OFC and bilateral amygdala (Fig. 4H). There were no statistically significant differences in the time of day of the dichotomized biomarker periods representing high and low SSS levels (Fig. 2s C,D). In addition, redefining the low gamma band (i.e. to 31–51 Hz) to assess the impact of the notch filter led to no changes in the study conclusions.

3.3. Local electrophysiology effects of stimulation mapping

To validate the association between the identified biomarker features and arousal, we next tested whether stimulation paradigms that modulated arousal also modulated these features. Using the biomarker features that were identified to be statistically significant across both patients (Fig. 4D, denoted by line and asterisks), we assessed the biomarker responses with respect to the most robust, wake-promoting stimulation site, i.e. right or left VC, and compared the response to a sleep-promoting site, i.e. 1Hz OFC stimulation (Fig. 5). Example spectrograms are constructed for select regions in response to 100Hz VC (Fig. 5A) and 1Hz OFC stimulation (Fig. 5C).

Across all patients, the post-stimulation spectral power was compared to the pre-stimulation power within relevant spectral bands (Fig. 5B,D). The group analysis of VC stimulation across all patients revealed increased spectral power in the high gamma power band within the left VC ($p = 0.019$), left SGC ($p = 0.037$), left OFC ($p = 0.011$), right OFC ($p = 0.016$), and right VC ($p = 0.029$), as well as increased spectral power in the low gamma power band within the right VC ($p = 0.033$) and right amygdala ($p = 0.038$). The change in spectral power within the low gamma band of the left VC was not statistically significant. In contrast to the effects of VC stimulation, 1Hz OFC stimulation did not elicit a change in the spectral power of any of the relevant sensing locations/frequency bands. Importantly, the increase in spectral power with VC stimulation in these regions/frequency bands are consistent with what would be predicted by the biomarker results, where increased power indicates increased wakefulness and decreased sleepiness.

4. Discussion

In this study, we present evidence that acute intracranial stimulation of corticolimbic sites modulates sleep-wake levels based on both subjective experience and behavior. Three novel targets whereby stimulation led to arousal effects were identified, including OFC, SGC, and most robustly, VC. Low frequency (1 Hz) stimulation of the OFC led to increased sleepiness, while high frequency (100 Hz) stimulation of the SGC, OFC, and VC led to increased wakefulness/arousal. Gamma frequency activity in a variety of subregions

was demonstrated to be associated with decreased sleepiness/increased wakefulness. The finding that a subset of these corticolimbic regions, which are broadly implicated in mood, motivation, inhibition, reward, and fear and currently investigated as targets for treatment-resistant depression [31, 38-40], modulates sleep-wake levels provides supporting evidence for shared circuitry between arousal and mood regulation in humans – a possible mechanism for the strong clinical and behavioral association of arousal and mood [5-7]. Additionally, the identification of novel targets highlights the feasibility of using neurostimulation in corticolimbic structures to modulate sleep-wake levels, potentially opening the door to novel neurostimulation strategies for disabling sleep-wake disorders.

We observed that stimulation of the bilateral VC yielded the most significant and robust increases in quantitative sleep-wake levels. Our findings expand upon and corroborate findings from an initial patient previously published by our group, suggesting a dose response of VC stimulation with clinician-scored arousal metrics [30]. Anecdotal experience with the initial patient, who subsequently underwent chronic responsive neurostimulation within the right VC [31] and reported symptoms of insomnia and disrupted sleep with right VC stimulation during evening hours, further reinforce this finding. These symptoms resolved when overnight VC stimulation was prevented. Indeed, the observations during the stimulation-mapping of this initial patient inspired methodologic changes to capture subjective experience of sleepiness-wakefulness in subsequent clinical trial participants, as presented in this study. Supplementary analysis with the initial patient is provided in Figs. 3s and 4s. In addition, our findings are consistent with other group's qualitative observations of increased engagement in conversation, energy, and awareness with therapeutic VC stimulation for TRD [41,42] and expand on such reports by providing quantitative measures of arousal levels.

While VC has been a target for DBS applications for depression [31,39,43,44], OCD [45], and other neuropsychiatric disorders, the physiological effects of VC stimulation remain poorly understood. VC stimulation is thought to activate traversing white matter tracts and their connected structures. Here, VC stimulation was identified to increase gamma activity in multiple brain regions (Fig. 5), including the bilateral VCs, amygdala, SGC, and OFC, suggesting a distributed and highly connected network associated with the VC subregion. Prominent tracts identified in models of depression and OCD include the anterior thalamic radiations connecting the anterior and medial nuclei of the thalamus to the frontal lobe [46,47], and the ventral tegmental area projection pathway (VTApp) connecting the VTA to the nucleus accumbens (NAc) and key frontal nodes including the subgenual cingulate (in some studies part of this pathway has been referred to as the superolateral branch of the medial forebrain bundle [47-50], though the existence of this structure as a discrete anatomic connection has recently been called into doubt [51]). Indeed, in our tractography results based on normative connectome data (Fig. 1B), models of tissue activated by stimulation at effective VC contacts were associated with fibers corresponding to both the anterior thalamic radiations and VTApp/MFB. In addition, structures near the VC, such as the bed nucleus of stria terminalis (BNST) and NAc, may be directly affected by the sphere of electrical stimulation.

In fact, the aforementioned corticolimbic structures associated with VC stimulation effects have recently been implicated in sleep-wake control by means of the mesolimbic dopamine pathways [16]. Modulation of dopaminergic VTA neurons have been demonstrated to sustain wakefulness, even during periods of high sleep drive [17,18,52]. Arousal effects of VTA stimulation have been traced to projections within the central amygdala, dorsolateral striatum, and most robustly within NAc, in which optogenetic and chemogenetic modulation of D1-expressing neurons promotes wakefulness in animal models [18,19]. D1 neurons within the NAc have additionally been observed to project to midbrain and lateral hypothalamus structures [19], thereby converging on classical arousal pathways, while D2 receptor-expressing GABAergic neurons within the NAc promote NREM [53]. As such, lesions within the NAc have eliminated wake-promoting effects of modafinil, a weak dopamine reuptake inhibitor and commonly used stimulant for excessive daytime sleepiness in a number of conditions including narcolepsy [54]. It is therefore possible that VC stimulation, leading to activation of VTApp/MFB and anterior thalamic radiations, yields behavioral increases in arousal indirectly via the modulation of connected structures (e.g. NAc, VTA) or directly via activation of the prefrontal cortex or the thalamus [55].

The neighboring BNST has additionally been associated with the activation of norepinephrine neurons within the locus coeruleus, lateral hypothalamus, and VTA, all wake-promoting regions [18,20]. Stimulation within the BNST has led to the rapid state transition to sustained wakefulness [56]. In addition, distinct activity and connectivity between the BNST and lateral hypothalamus lead to hypocretin/orexin expression and may be play a role in driving opposing emotional states [20,57]. An alternative mechanism of VC stimulation therefore includes the activation of neighboring, wake-promoting subcortical structures, i.e. the BNST, included in the theoretical volume of activated tissue.

In our study, SGC stimulation demonstrated a moderate response in wakefulness, which may relate to its connectivity to structures involved in visceromotor activity and recent findings demonstrating an association with autonomic arousal [58,59]. The arousal response within the SGC was overall less robust, which may relate to the variability in the identified fiber tracts recruited based on electrode positioning between the two patients (Fig. 1B). Finally, the OFC behavioral responses were also less robust, which may relate to the relatively large territory of the OFC and the associated variation across participants in electrode location and stimulation, spanning the medial to lateral OFC. Connectivity analysis revealed fibers corresponding to a branch of the anterior thalamic radiations, i.e. inferior thalamic peduncle, associated with effective OFC stimulation sites in Patient 1 and may also play a role in the modulation of sleep-wake levels via the direct activation of thalamus [55]. It is also possible that the heterogeneity observed in both regions reflect a more complex relationship with arousal, such as state dependence [30]. Given the heterogeneity of responses and tracts recruited, further studies with more patients are required to elucidate which specific fiber tract(s) associated with SGC and OFC stimulation promote wakefulness. Further studies are also required to assess the differences in arousal responses between contralateral regions, for which systematic mapping was limited by statistical power due to the nature of the study to advance toward candidate mood-specific stimulation targets.

In addition to differential effects across regions, our findings indicate that the frequency of stimulation may have differential effects on sleep-wake responses. While low and high frequency intracranial stimulation of OFC have been identified to yield specific antidepressant effects in a prior study [30], we demonstrate that 1Hz OFC stimulation led to increased sleepiness, while 100Hz OFC stimulation led to increased wakefulness. The differential frequency-dependent findings were similarly recapitulated with the initial patient with a subset of outcome measures (Fig. 3s). Stimulation at low versus high frequencies has been identified to selectively modulate excitatory and inhibitory neural populations [60-62], which likely gives rise to the variable clinical effects. Prior work has also demonstrated that low frequency stimulation is associated with presynaptic activation and high frequency activity is associated with synaptic depression [63,64]. Indeed, dating back to early work from the 1940s, stimulation within the classical subcortical arousal circuitry has also revealed frequency-specific effects, including within the reticular activating system and thalamus [65-67]. For instance, high frequency electrical stimulation of the reticular activating system, central thalamus or intralaminar nuclei within animal models has been demonstrated to evoke cortical activation patterns of desynchronization and behavioral arousal [66,68]. On the other hand, low frequency stimulation within these classical regions has led to decreased neural firing with spike-wave absence seizure activity or slow-wave and spindle activity, associated with behavioral arrest, drowsiness, and/or loss of consciousness [67,69]. The opposing effects on sleepiness induced here by high and low frequency OFC stimulation suggest that stimulus parameter tuning for neuromodulation of corticolimbic sites will be essential for potential future therapeutic applications.

Although sleepiness is known to be associated with a decrease in higher frequency activity (alpha, beta, low gamma and high gamma) and an increase in delta and theta power in scalp EEG data [70-72], the correlates of sleepiness within intracranial targets have not been systematically studied. Importantly, in our biomarker analysis, subjective sleepiness was found to correlate with specific spectral power features within the SGC, VC, amygdala, and OFC, providing further evidence for the distributed effects of the arousal network, including within corticolimbic regions [8,9,73]. The most prominent biomarker features were increases in low and high gamma frequency activity, which were correlated with increased wakefulness, while increased lower frequency activity was associated with increased sleepiness, mirroring findings from surface EEG. Decreases in gamma activity with subjective sleepiness across all recorded regions suggest that perceived sleepiness is associated with broad changes in brain activity affecting both cortical and subcortical structures. These biomarker features are consistent with prior studies that have demonstrated that gamma frequency activity across broad cortical regions correlates with sleep-wake states, as well as attention and cognitive tasks [74-77]. Furthermore, these findings are relevant for future efforts involving intracranial recordings and stimulation. Specifically, our recent work [30], revealing that the antidepressant effects of intracranial stimulation are dependent on arousal level, suggests that it may be important to characterize and control for arousal as part of optimal treatment delivery.

Our findings extend prior deep-brain stimulation studies in humans indicating that arousal level can be modulated with direct neural stimulation [25-27] by expanding both the patient population and the target selection. Given that our study is performed in participants without

significant neural injury or neurodegeneration, the participants were able to articulate their experiences and provide more sensitive outcome measures of sleepiness and energy to facilitate comparison between different stimulation targets. Prior studies of sleep-wake effects in patients with advanced PD and severe sleep disturbances also revealed that chronic low stimulation of the PPN led to decreased daytime sleepiness and improved sleep quality [29], whereas high frequency stimulation induced NREM sleep [28]. These findings reinforce frequency-dependent effects of stimulation, such that changes in stimulation frequency can yield opposing effects, as seen in our study with low and high frequency OFC stimulation. Finally, we highlight that a unique aspect of this study is that, unlike prior stimulus-response mapping work, primarily carried out in those with epilepsy, we had access to subjects without epilepsy undergoing a stimulation-mapping paradigm with bilateral corticolimbic implants (including the VC), thereby eliminating confounds related to anti-seizure medications or epileptiform activity.

This study has limitations. 1) Our findings in patients with treatment-resistant depression may not be generalizable to other patient populations. Further efforts to investigate sleep-wake responses in patients without an underlying mood disorder will be important to assess any contribution from potentially altered emotional regulation networks. 2) This study is limited to two patients (with supporting data from a third patient in the Supplementary Materials). An important distinction from other intracranial mapping studies is that the subjects discussed in this study underwent an intensive 10 d inpatient monitoring period with continuous recordings and comprehensive stimulation mapping, enabling a personalized, detailed, and robust evaluation. In contrast, intracranial mapping studies that leverage patients undergoing EMU monitoring are limited to a small number of stimulation tests, spread across many patients (often due to the limited testing time). In our study, a large number of stimulation and biomarker recordings were collected per individual, leading to findings that were statistically powered within each patient. Future efforts to continue to expand this analysis to a larger cohort of patients is indicated and underway. 3) Finally, limited frequencies of stimulation were tested (1Hz in OFC and 100 Hz in all other sites, i.e. frequencies optimized in depression studies); further exploration of different stimulation frequencies is required for the optimization for arousal responses and will be the subject of future work.

In summary, our work presents new evidence in human participants that stimulation of corticolimbic regions modulates subjective sleep-wake level and that electrophysiologic biomarkers within corticolimbic sites correlate with changes in sleep-wake levels. Three novel targets – VC, SGC, and OFC – were implicated in mediating sleep-wake levels. Crucially, these findings indicate a broad overlap in the circuitry underlying mood and arousal, which may ultimately explain the strong behavioral and clinical links between mood and arousal [6,7]. In addition, these findings open the door to new treatment targets and the consideration of therapeutic brain stimulation for sleep-wake disorders [78], such as idiopathic hypersomnia, a condition characterized by excessive daytime sleepiness. Future efforts to map brain regions involved in the extended arousal circuitry will be critical for the ongoing identification of novel treatment targets for the future application of neurostimulation for intractable sleep-wake disorders.

Supplementary Material

Refer to Web version on PubMed Central for supplementary material.

Acknowledgements

Code availability

The computer code that supports the findings of this study are available from the corresponding author upon reasonable request.

References

[1]. Saper CB, Fuller PM. Wake-sleep circuitry: an overview. Curr Opin Neurobiol 2017;44:186. 10.1016/J.CONB.2017.03.021. [PubMed: 28577468]

[2]. Ashbrook LH, Krystal AD, Fu YH, Ptáek LJ. Genetics of the human circadian clock and sleep homeostat. Neuropsychopharmacology 2020;45(1):45–54. 10.1038/S41386-019-0476-7. [PubMed: 31400754]

[3]. Wright KP, Lowry CA, leBourgeois MK. Circadian and wakefulness-sleep modulation of cognition in humans. Front Mol Neurosci 2012;0(APRIL):50. 10.3389/FNMOL.2012.00050/BIBTEX.

[4]. Konjarski M, Murray G, Lee VV, Jackson ML. Reciprocal relationships between daily sleep and mood: a systematic review of naturalistic prospective studies. Sleep Med Rev 2018;42:47–58. 10.1016/J.SMRV.2018.05.005. [PubMed: 30404728]

[5]. Ptáek LJ, Fu YH, Krystal AD. Sleep and mood: chicken or egg? Biol Psychiatr 2016;80(11):810–1. 10.1016/J.BIOPSYCH.2016.09.012.

[6]. Becker PM. Treatment of sleep dysfunction and psychiatric disorders. Curr Treat Options Neurol 2006;8(5):367–75. 10.1007/S11940-006-0026-6. [PubMed: 16901376]

[7]. Alvaro PK, Roberts RM, Harris JK. A systematic review assessing bidirectionality between sleep disturbances, anxiety, and depression. Sleep 2013;36(7):1059–68. 10.5665/SLEEP.2810. [PubMed: 23814343]

[8]. Munn BR, Müller EJ, Wainstein G, Shine JM. The ascending arousal system shapes neural dynamics to mediate awareness of cognitive states. Nat Commun 2021;12 (1):1–9. 10.1038/s41467-021-26268-x. 2021 121. [PubMed: 33397941]

[9]. Petersen SE, Sporns O. Brain networks and cognitive architectures. Neuron 2015;88(1):207–19. 10.1016/j.neuron.2015.09.027. [PubMed: 26447582]

[10]. Sporns O. Network attributes for segregation and integration in the human brain. Curr Opin Neurobiol 2013;23(2):162–71. 10.1016/j.conb.2012.11.015. [PubMed: 23294553]

[11]. Brown EN, Purdon PL, Van Dort CJ. General anesthesia and altered states of arousal: a systems neuroscience analysis. 2011. 10.1146/ANNUREV-NEURO-060909-153200. 34:601–628.

[12]. Brown RE, Basheer R, McKenna JT, Strecker RE, McCarley RW. Control of sleep and wakefulness. Physiol Rev 2012;92(3):1087. 10.1152/PHYSREV.00032.2011. [PubMed: 22811426]

[13]. Feindel W, Gloor P. Comparison of electrographic effects of stimulation of the amygdala and brain stem reticular formation in cats. Electroencephalogr Clin Neurophysiol 1954;6(C):389–402. 10.1016/0013-4694(54)90053-X. [PubMed: 13200410]

[14]. Jasper H, Pertuisset B, Flanigin H. Eeg and cortical electrograms in patients with temporal lobe seizures. Arch Neurol Psychiatr 1951;65(3):272–90. 10.1001/ARCHNEURPSYC.1951.02320030009002. [PubMed: 14810279]

[15]. Llinás RR, Paré D. Of dreaming and wakefulness. Neuroscience 1991;44(3):521–35. 10.1016/0306-4522(91)90075-Y. [PubMed: 1754050]

[16]. Oishi Y, Lazarus M. The control of sleep and wakefulness by mesolimbic dopamine systems. Neurosci Res 2017;118:66–73. 10.1016/j.neures.2017.04.008. [PubMed: 28434991]

[17]. Oishi Y, Suzuki Y, Takahashi K, et al. Activation of ventral tegmental area dopamine neurons produces wakefulness through dopamine D2-like receptors in mice. Brain Struct Funct 2017;222(6):2907–15. 10.1007/s00429-017-1365-7. [PubMed: 28124114]

[18]. Eban-Rothschild A, Rothschild G, Giardino WJ, Jones JR, De Lecea L. VTA dopaminergic neurons regulate ethologically relevant sleep-wake behaviors. Nat Neurosci 2016;19(10):1356–66. 10.1038/nn.4377. [PubMed: 27595385]

[19]. Luo YJ, Li YD, Wang L, et al. Nucleus accumbens controls wakefulness by a subpopulation of neurons expressing dopamine D1 receptors. Nat Commun 2018;9 (1):1–17. 10.1038/s41467-018-03889-3. [PubMed: 29317637]

[20]. Giardino WJ, Pomrenze MB. Extended amygdala neuropeptide circuitry of emotional arousal: waking up on the wrong side of the bed nuclei of stria terminalis. Front Behav Neurosci 2021;15:6. 10.3389/FNBEH.2021.613025/BIBTEX.

[21]. Knutson B, Greer SM. Anticipatory affect: neural correlates and consequences for choice. Philos Trans R Soc B Biol Sci 2008;363(1511):3771. 10.1098/RSTB.2008.0155.

[22]. Russell JA. A circumplex model of affect. J Pers Soc Psychol 1980;39(6):1161–78. 10.1037/H0077714.

[23]. Watson D, Tellegen A. Toward a consensual structure of mood. Psychol Bull 1985;98(2):219–35. 10.1037/0033-2909.98.2.219. [PubMed: 3901060]

[24]. Barrett LF. Discrete emotions or dimensions? The role of valence focus and arousal focus. 2010. 10.1080/026999398379574. 12(4):579–599.

[25]. Schiff ND, Giacino JT, Kalmar K, et al. Behavioural improvements with thalamic stimulation after severe traumatic brain injury. Nature 2007;448(7153):600–3. 10.1038/nature06041. [PubMed: 17671503]

[26]. Kundu B, Brock AA, Englot DJ, Butson CR, Rolston JD. Deep brain stimulation for the treatment of disorders of consciousness and cognition in traumatic brain injury patients: a review. Neurosurg Focus 2018;45(2):E14. 10.3171/2018.5.FOCUS18168.

[27]. Gummadavelli A, Kundishora AJ, Willie JT, et al. Neurostimulation to improve level of consciousness in patients with epilepsy. Neurosurg Focus 2015;38(6). 10.3171/2015.3.FOCUS1535.

[28]. Arnulf I, Ferraye M, Fraix V, et al. Sleep induced by stimulation in the human pedunculopontine nucleus area. Ann Neurol 2010;67(4):546–9. 10.1002/ANA.21912. [PubMed: 20437591]

[29]. Peppe A, Pierantozzi M, Baiamonte V, et al. Deep brain stimulation of pedunculopontine tegmental nucleus: role in sleep modulation in advanced Parkinson disease patients—one-year follow-up. Sleep 2012;35(12):1637. 10.5665/SLEEP.2234. [PubMed: 23204606]

[30]. Scangos KW, Makhoul GS, Sugrue LP, Chang EF, Krystal AD. State-dependent responses to intracranial brain stimulation in a patient with depression. Nat Med 2021;27(2):229–31. 10.1038/s41591-020-01175-8. [PubMed: 33462446]

[31]. Scangos KW, Khambhati AN, Daly PM, et al. Closed-loop neuromodulation in an individual with treatment-resistant depression. Nat Med 2021;27(10):1696–700. 10.1038/s41591-021-01480-w. 2021 2710. [PubMed: 34608328]

[32]. Horn A, Li N, Dembek TA, et al. Lead-DBS v2: towards a comprehensive pipeline for deep brain stimulation imaging. Neuroimage 2019;184:293–316. 10.1016/J.NEUROIMAGE.2018.08.068. [PubMed: 30179717]

[33]. Fonov V, Evans A, McKinstry R, Almli C, Collins D. Unbiased nonlinear average age-appropriate brain templates from birth to adulthood. Neuroimage 2009;47:S102. 10.1016/S1053-8119(09)70884-5.

[34]. Horn A, Neumann WJ, Degen K, Schneider GH, Kühn AA. Toward an electrophysiological "sweet spot" for deep brain stimulation in the subthalamic nucleus. Hum Brain Mapp 2017;38(7):3377–90. 10.1002/HBM.23594. [PubMed: 28390148]

[35]. Dembek TA, Barbe MT, Åström M, et al. Probabilistic mapping of deep brain stimulation effects in essential tremor. Neuroimage Clin 2016;13:164–73. 10.1016/J.NICL.2016.11.019. [PubMed: 27981031]

[36]. Hoddes E, Zarcone V, Smythe H, Phillips R, Dement WC. Quantification of sleepiness: a new approach. Psychophysiology 1973;10(4):431–6. 10.1111/J.1469-8986.1973.TB00801.X. [PubMed: 4719486]

[37]. Fan JM, Khambhati AN, Sellers KK, et al. Epileptiform discharges triggered with direct electrical stimulation for treatment-resistant depression: factors that modulate risk and treatment considerations. Brain Stimul Basic, Transl Clin Res Neuromodulation. 2023;0(0). 10.1016/J.BRS.2023.02.006.

[38]. Mayberg HS, Riva-Posse P, Crowell AL. Deep brain stimulation for depression: keeping an eye on a moving target. JAMA Psychiatr 2016;73(5):439–40. 10.1001/JAMAPSYCHIATRY.2016.0173.

[39]. Dougherty DD, Rezai AR, Carpenter LL, et al. A randomized sham-controlled trial of deep brain stimulation of the ventral capsule/ventral striatum for chronic treatment-resistant depression. Biol Psychiatr 2015;78(4):240–8. 10.1016/j.biopsych.2014.11.023.

[40]. Rao VR, Sellers KK, Wallace DL, et al. Direct electrical stimulation of lateral orbitofrontal cortex acutely improves mood in individuals with symptoms of depression. Curr Biol 2018;28(24):3893–3902.e4. 10.1016/j.cub.2018.10.026. [PubMed: 30503621]

[41]. Malone DA, Dougherty DD, Rezai AR, et al. Deep brain stimulation of the ventral capsule/ventral striatum for treatment-resistant depression. Biol Psychiatr 2009;65(4):267–75. 10.1016/J.BIOPSYCH.2008.08.029.

[42]. Schlaepfer TE, Bewernick BH, Kayser S, Mädler B, Coenen VA. Rapid effects of deep brain stimulation for treatment-resistant major depression. Biol Psychiatr 2013;73(12):1204–12. 10.1016/J.BIOPSYCH.2013.01.034.

[43]. Bergfeld IO, Mantione M, Hoogendoorn MLC, et al. Deep brain stimulation of the ventral anterior limb of the internal capsule for treatment-resistant depression. JAMA Psychiatr 2016;73(5):456–64. 10.1001/jamapsychiatry.2016.0152.

[44]. Mayberg HS, Riva-Posse P, Crowell AL. Deep brain stimulation for depression: keeping an eye on a moving target. JAMA Psychiatr 2016;73(5):439–40. 10.1001/jamapsychiatry.2016.0173.

[45]. Greenberg BD, Gabriels LA, Malone DA, et al. Deep brain stimulation of the ventral internal capsule/ventral striatum for obsessive-compulsive disorder: worldwide experience. Mol Psychiatr 2008;15(1):64–79. 10.1038/mp.2008.55. 2010 151.

[46]. Baldermann JC, Melzer C, Zapf A, et al. Connectivity profile predictive of effective deep brain stimulation in obsessive-compulsive disorder. Biol Psychiatr 2019;85(9):735–43. 10.1016/J.BIOPSYCH.2018.12.019.

[47]. Li N, Baldermann JC, Kibleur A, et al. A unified connectomic target for deep brain stimulation in obsessive-compulsive disorder. Nat Commun 2020;11(1). 10.1038/S41467-020-16734-3.

[48]. Coenen VA, Bewernick BH, Kayser S, et al. Superolateral medial forebrain bundle deep brain stimulation in major depression: a gateway trial. Neuropsychopharmacology 2019;44(7):1224–32. 10.1038/S41386-019-0369-9. 2019 447. [PubMed: 30867553]

[49]. Schlaepfer TE, Bewernick BH, Kayser S, Hurlemann R, Coenen VA. Deep brain stimulation of the human reward system for major depression–rationale, outcomes and outlook. Neuropsychopharmacology 2014;39(6):1303–14. 10.1038/NPP.2014.28. [PubMed: 24513970]

[50]. Coenen VA, Schlaepfer TE, Sajonz B, et al. Tractographic description of major subcortical projection pathways passing the anterior limb of the internal capsule. Corticopetal organization of networks relevant for psychiatric disorders. Neuroimage Clin 2020;25. 10.1016/J.NICL.2020.102165.

[51]. Haber SN, Yendiki A, Jbabdi S. Four deep brain stimulation targets for obsessive-compulsive disorder: are they different? Biol Psychiatr 2021;90(10):667–77. 10.1016/J.BIOPSYCH.2020.06.031.

[52]. Dahan L, Astier B, Vautrelle N, Urbain N, Kocsis B, Chouvet G. Prominent burst firing of dopaminergic neurons in the ventral tegmental area during paradoxical sleep. Neuropsychopharmacology 2007;32(6):1232–41. 10.1038/SJ.NPP.1301251. [PubMed: 17151599]

[53]. Oishi Y, Xu Q, Wang L, et al. Slow-wave sleep is controlled by a subset of nucleus accumbens core neurons in mice. Nat Commun 2017;8(1):1–12. 10.1038/S41467-017-00781-4. 2017 81. [PubMed: 28232747]

[54]. Qiu MH, Liu W, Qu WM, Urade Y, Lu J, Huang ZL. The role of nucleus accumbens core/shell in sleep-wake regulation and their involvement in modafinil-induced arousal. PLoS One 2012;7(9). 10.1371/JOURNAL.PONE.0045471.

[55]. Redinbaugh MJ, Phillips JM, Kambi NA, et al. Thalamus modulates consciousness via layer-specific control of cortex. Neuron 2020;106(1):66–75.e12. 10.1016/J.NEURON.2020.01.005. [PubMed: 32053769]

[56]. Kodani S, Soya S, Sakurai T. Optogenetic manipulation of neural circuits during monitoring sleep/wakefulness states in mice. J Vis Exp 2019;2019(148). 10.3791/58613.

[57]. Giardino WJ, Eban-Rothschild A, Christoffel DJ, Li S Bin, Malenka RC, de Lecea L. Parallel circuits from the bed nuclei of stria terminalis to the lateral hypothalamus drive opposing emotional states. Nat Neurosci 2018;21(8):1084–95. 10.1038/s41593-018-0198-x. 2018 218. [PubMed: 30038273]

[58]. Rudebeck PH, Putnam PT, Daniels TE, et al. A role for primate subgenual cingulate cortex in sustaining autonomic arousal. Proc Natl Acad Sci U S A 2014;111(14):5391–6. 10.1073/PNAS.1317695111/-/DCSUPPLEMENTAL. [PubMed: 24706828]

[59]. Alexander L, Wood CM, Gaskin PLR, et al. Over-activation of primate subgenual cingulate cortex enhances the cardiovascular, behavioral and neural responses to threat. Nat Commun 2020;11(1):1–14. 10.1038/s41467-020-19167-0. 2020 111. [PubMed: 31911652]

[60]. Mahmud M, Vassanelli S. Differential modulation of excitatory and inhibitory neurons during periodic stimulation. Front Neurosci 2016;10(FEB). 10.3389/FNINS.2016.00062.

[61]. Lee KY, Bae C, Lee D, et al. Low-intensity, kilohertz frequency spinal cord stimulation differently affects excitatory and inhibitory neurons in the rodent superficial dorsal Horn. Neuroscience 2020;428:132–9. 10.1016/J.NEUROSCIENCE.2019.12.031. [PubMed: 31917342]

[62]. Mohan UR, Watrous AJ, Miller JF, et al. The effects of direct brain stimulation in humans depend on frequency, amplitude, and white-matter proximity. Brain Stimul 2020;13(5):1183–95. 10.1016/J.BRS.2020.05.009. [PubMed: 32446925]

[63]. Varela JA, Song S, Turrigiano GG, Nelson SB. Differential depression at excitatory and inhibitory synapses in visual cortex. J Neurosci 1999;19(11):4293. 10.1523/JNEUROSCI.19-11-04293.1999. [PubMed: 10341233]

[64]. Liu LD, Prescott IA, Dostrovsky JO, Hodaie M, Lozano AM, Hutchison WD. Frequency-dependent effects of electrical stimulation in the globus pallidus of dystonia patients. J Neurophysiol 2012;108(1):5–17. 10.1152/JN.00527.2011/ASSET/IMAGES/LARGE/Z9K0131214020007.JPEG. [PubMed: 22457462]

[65]. Jasper H. Diffuse projection systems: the integrative action of the thalamic reticular system. Electroencephalogr Clin Neurophysiol 1949;1(1–4):405–20. 10.1016/0013-4694(49)90213-8. [PubMed: 18421831]

[66]. Moruzzi G, Magoun HW. Brain stem reticular formation and activation of the EEG. Electroencephalogr Clin Neurophysiol 1949;1(1–4):455–73. 10.1016/0013-4694(49)90219-9. [PubMed: 18421835]

[67]. Liu J, Lee HJ, Weitz AJ, et al. Frequency-selective control of cortical and subcortical networks by central thalamus. Elife 2015;4(DECEMBER2015). 10.7554/ELIFE.09215.001.

[68]. Schiff ND. Central thalamic contributions to arousal regulation and neurological disorders of consciousness. Ann N Y Acad Sci 2008;1129(1):105–18. 10.1196/ANNALS.1417.029. [PubMed: 18591473]

[69]. Moruzzi G. The sleep-waking cycle. Ergeb Physiol 1972;64:1–165. 10.1007/3-540-05462-6_1. [PubMed: 4340664]

[70]. Hubbard J, Gent TC, Hoekstra MMB, et al. Rapid fast-delta decay following prolonged wakefulness marks a phase of wake-inertia in NREM sleep. Nat Commun 2020;11(1):1–16. 10.1038/s41467-020-16915-0. 2020 111. [PubMed: 31911652]

[71]. Åkerstedt T, Gillberg M. Subjective and objective sleepiness in the active individual. 2009. 10.3109/00207459008994241. 52(1-2):29–37.

[72]. De Gennaro L, Marzano C, Veniero D, et al. Neurophysiological correlates of sleepiness: a combined TMS and EEG study. Neuroimage 2007;36(4):1277–87. 10.1016/J.NEUROIMAGE.2007.04.013. [PubMed: 17524675]

[73]. Shine JM, Müller EJ, Munn B, Cabral J, Moran RJ, Breakspear M. Computational models link cellular mechanisms of neuromodulation to large-scale neural dynamics. Nat Neurosci 2021;24(6):765–76. 10.1038/s41593-021-00824-6. 2021 246. [PubMed: 33958801]

[74]. Gross DW, Gotman J. Correlation of high-frequency oscillations with the sleep– wake cycle and cognitive activity in humans. Neuroscience 1999;94(4):1005–18. 10.1016/S0306-4522(99)00343-7. [PubMed: 10625043]

[75]. Tiitinen HT, Sinkkonen J, Reinikainen K, Alho K, Lavikainen J, Näätänen R. Selective attention enhances the auditory 40-Hz transient response in humans. Nature 1993;364(6432):59–60. 10.1038/364059A0. [PubMed: 8316297]

[76]. Lindens RD, Campbell KB, Hamel G, Picton TW. Human auditory steady state evoked potentials during sleep. Ear Hear 1985;6(3):167–74. 10.1097/00003446-198505000-00008. [PubMed: 4007303]

[77]. Maloney KJ, Cape EG, Gotman J, Jones BE. High-frequency gamma electroencephalogram activity in association with sleep-wake states and spontaneous behaviors in the rat. Neuroscience 1997;76(2):541–55. 10.1016/S0306-4522(96)00298-9. [PubMed: 9015337]

[78]. Venner A, Todd WD, Fraigne JJ, et al. Newly identified sleep-wake and circadian circuits as potential therapeutic targets. Sleep 2019;42(5). 10.1093/SLEEP/ZSZ023.
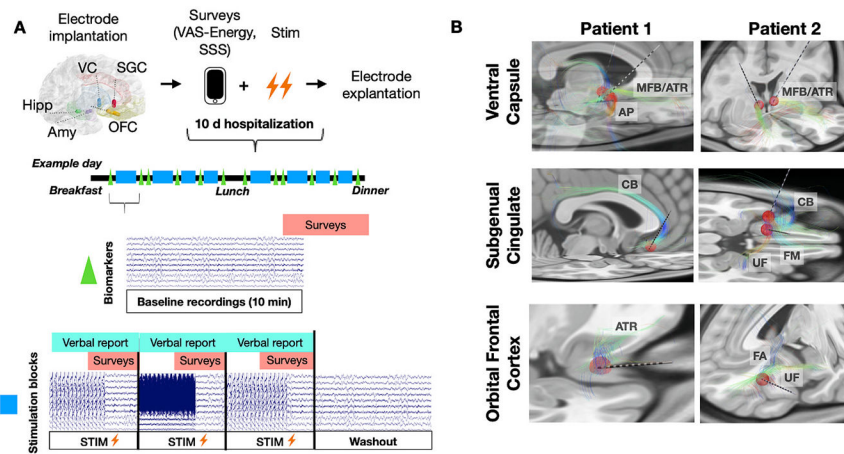
Fig. 1. Overview of experimental methodology and imaging of implantation sites.
A) Following electrode implantation, each patient underwent an intensive 10 d inpatient monitoring period, in which biomarker recordings and stimulation testing were performed. Biomarker recordings comprised of 10 min of resting state activity, followed by survey completion. During stimulation testing, patients provided spontaneous verbal reports of any sensations and survey responses were completed at the end of the stimulation period. Survey assessments included the SSS and VAS-Energy scores. In addition, bedside clinical arousal scores were recorded in response to stimulation. We note that the represented neural signal is a truncated duration of time for each block and is intended only for the illustration purposes of the stimulation block design (see Fig. 1s for a scaled representation). B) Structural connectivity analysis for both patients based on seeding the normative connectome with the volume of tissue predicted to be activated by stimulation at representative stimulation sites within the VC (*top*). SGC (*middle*), and OFC (*bottom*). Stimulation at VC contacts is associated with fibers corresponding to the medial forebrain bundle (MFB), anterior thalamic radiations (ATR), and ansa peduncularis (AP). Stimulation at SGC contacts is associated with fibers corresponding to the forceps minor (FM), cingulum bundle (CB), and uncinate fasciculus (UF). Stimulation at OFC contacts is associated with fibers corresponding to the ventral component of the ATR, UF, and frontal asalant (FA) tracts. Red spheres represent the location and volume of tissue activated used for fiber tracking in the normative connectome. Coloration of tracts follows conventional coding, i.e. right-left (red), anterior-posterior (green), and superior-inferior (blue) fiber directions.
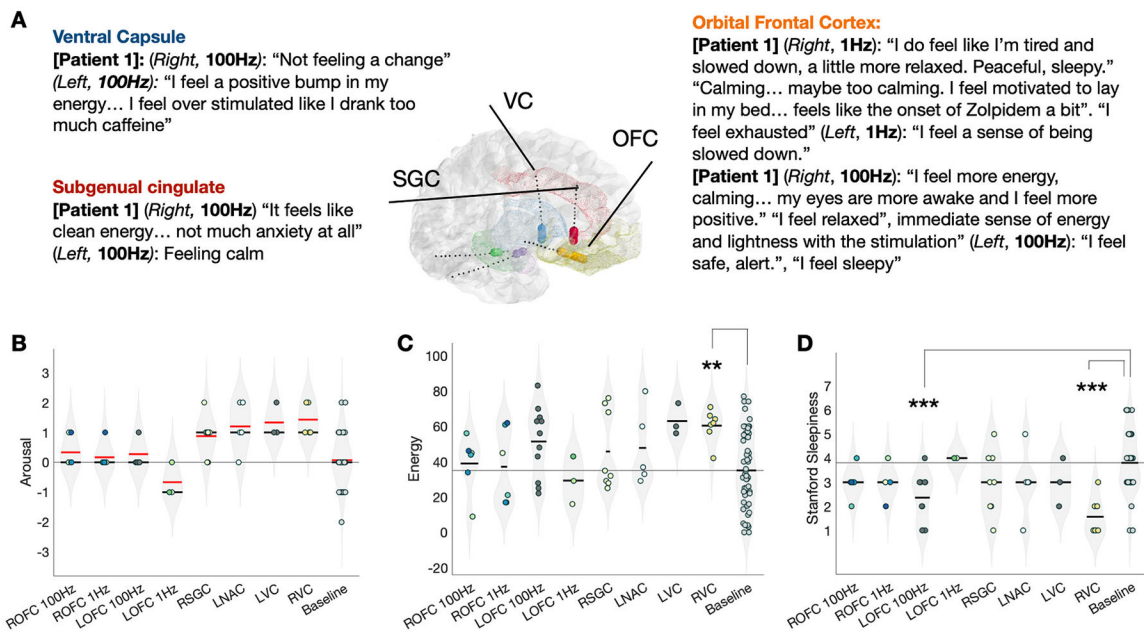
Fig. 2. Example behavioral reports and survey responses from an individual patient.
A) Example spontaneous verbal reports associated with stimulation at the specified
regions for Patient 1. B-D) Behavioral responses from Patient 2 for arousal, energy, and
SSS, respectively, illustrate a statistically significant increase in energy and reduction in
sleepiness in response to right VC 100Hz stimulation and a reduction in sleepiness in
response to left OFC 100Hz stimulation. Different electrode bipolar pairs within a region of
stimulation are uniquely color-coded within each violin plot. Abbreviations: R = right; L =
left; OFC = orbital frontal cortex; SGC = subgenual cingulate, NAC = nucleus accumbens,
VC = ventral capsule.
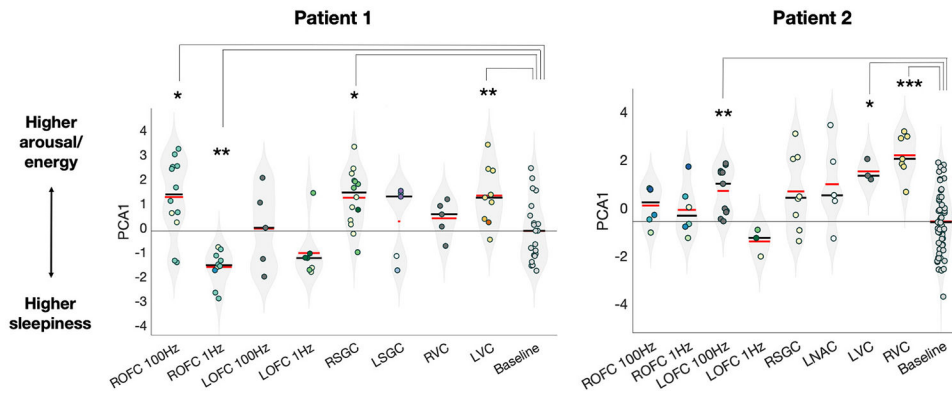
Fig. 3.
Behavioral effects of arousal to regional stimulation across in both patients. Stimulation response quantified by the summary metric (i.e. first dimension of PCA across the three behavioral assessments) in Patients 1 (*left)* and 2 (*right*), respectively. Different electrode bipolar pairs within a region of stimulation are uniquely color-coded within each violin plot.
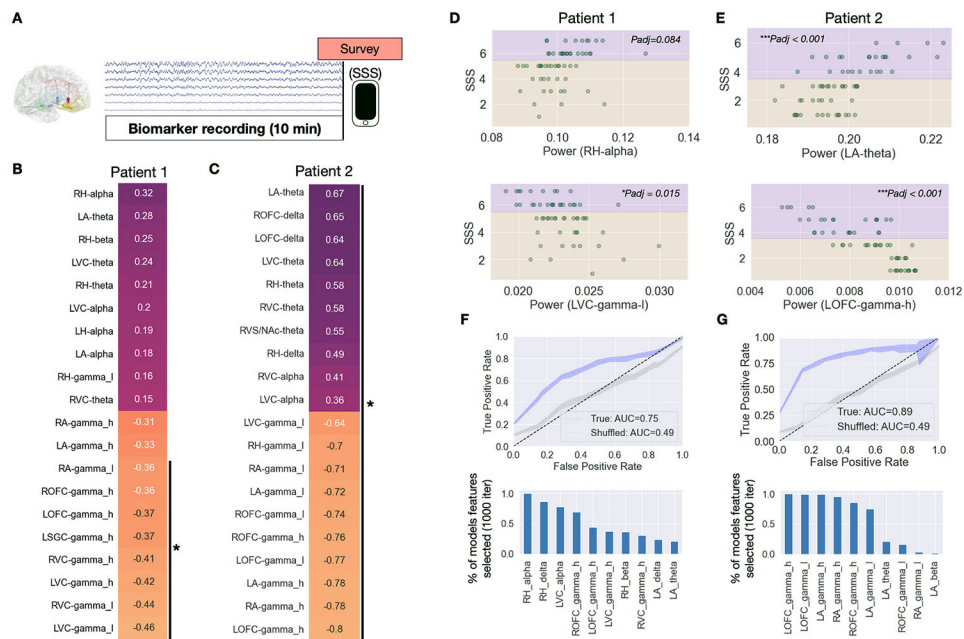
Fig. 4. Electrophysiologic biomarkers of sleepiness across both patients.
A) Electrophysiology for biomarker analysis was obtained from the resting-state periods preceding survey completion. B) Top 10 features with highest positive and negative correlations with SSS for Patient 1. Correlations that were statistically significant following multiple comparison testing across regions are indicated by the line and asterisks (*right*). C) Same as B, but for Patient 2. D) Example of the highest positive and negative correlations between SSS and candidate electrophysiologic features, e.g. relative power in the alpha band of the right hippocampus (*top*) and low gamma band of the left ventral capsule (*bottom*). Purple and orange background shading represent the high and low sleepiness state cut-offs used for logistic regression classification. E) Same as D, but for Patient 2, illustrating the relationship between SSS and relative power in the theta band of the left amygdala (*top*) and high gamma band of the left OFC (*bottom*). F) ROC curves representing the best average model from cross-validated logistic regressions using six features (*top*) with AUC 0.75. Demonstration of top model features used in multivariate logistic regression *(bottom)*, quantified by percent of models in which features were selected from cross-validated 1000 iterations. G) Same as F, but for Patient 2 for whom the best logistic regression model achieved an AUC of 0.89.
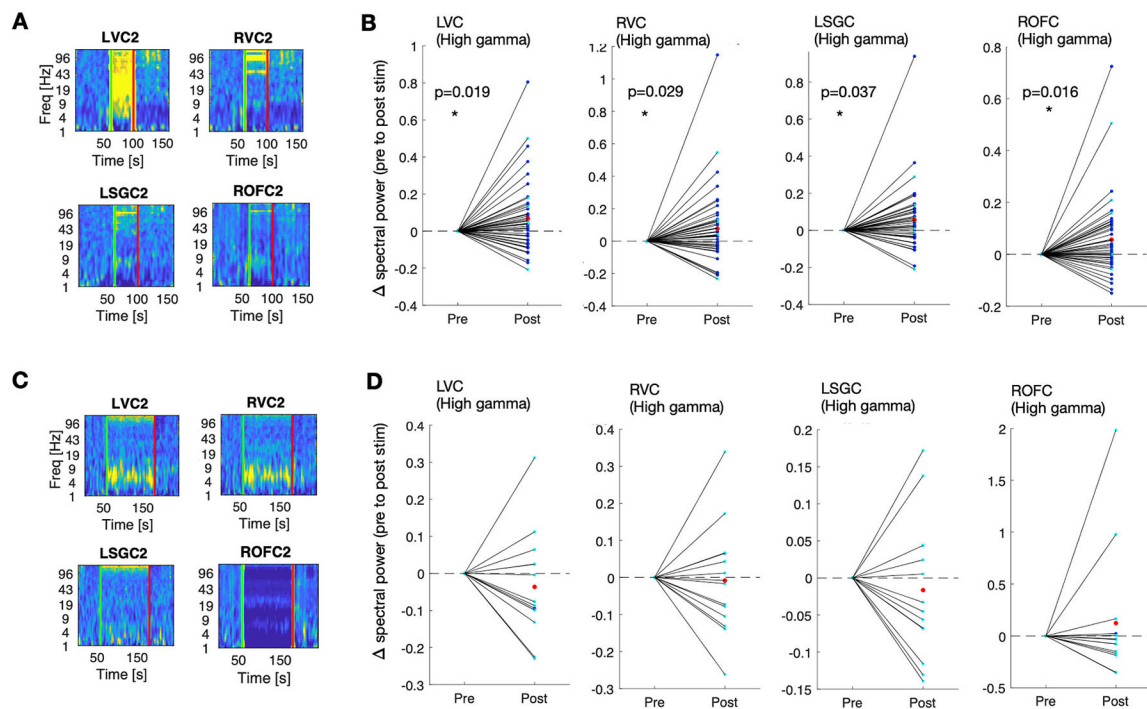
Fig. 5. Effects of regional stimulation on shared electrophysiologic biomarkers of sleepiness.
A) Example local spectrograms before, during, and after stimulation between the left VC 2 and 3 channels at 100Hz, 2 mA. Green and red lines denote onset and offset of stimulation, respectively. Visualized spectrograms represent the electrophysiology observed from the left VC (*top left*), right VC (*top right*), left SGC (*bottom left*) and right OFC (*bottom right*) contacts. B) Changes from pre-stim to post-stim z-scored spectral power for identified biomarkers of sleepiness aggregated across both patients, in response to VC stimulation (cyan dots, patient 1; blue dots, patient 2; red dots, group mean). A subset of the group biomarker responses to stimulation are presented, including high gamma power within the left VC, right VC, left SGC, and right OFC. C) Example local spectrograms during stimulation between the right OFC 2 and 9 channels at 1Hz, 3 mA. Visualized spectrograms represent the electrophysiology from the same contacts as in A. D) As in B, change from pre-stim to post-stim high gamma power within the left VC, right VC, left SGC, and right OFC, in response to 1Hz OFC stimulation. No statistically significant responses were observed in the low or high gamma power with respect to 1Hz OFC stimulation.